Composition and Formation Mechanism of Brown Carbon: Identification and **Quantification of Phenolic Precursors** Md. Al-amin Hossen¹, Mehedi Hasan Shakil¹, Md. Fahim Ehasan², Abu Rayhan Mohammad Tareq², Abdus Salam^{1*} ¹Department of Chemistry, Faculty of Science, University of Dhaka, Dhaka-1000, Bangladesh ²Environmental and Organic Chemistry Laboratory, Chemistry Division, Atomic Energy Centre Dhaka, Bangladesh *Corresponding author: asalam@gmail.com; asalam@du.ac.bd

25 Abstract

Light-absorbing organic carbon, collectively known as brown carbon (BrC), significantly influence climate and air quality, particularly in urban environments like Dhaka, Bangladesh. Despite their significance, the contributions and transformation pathways of phenolic compounds—major precursors of brown carbon (BrC)—are still insufficiently understood in the South Asian megacities. This study addresses this gap by investigating the surface morphology of PM2.5, quantifying seven phenolic BrC precursors, and exploring the aqueous-phase formation pathway of nitrophenols at two urban sites (Dhaka South and Dhaka North) from July 2023 to January 2024. Phenolic compounds, including phenol, methylphenols, methoxyphenol, hydroxyphenol, and nitrophenol were identified and quantified using gas chromatography-flame ionization detection (GC-FID). PM2.5 surface morphology and elemental composition were analyzed via Field Emission Scanning Electron Microscopy – Energy Dispersive X-ray Spectroscopy (FESEM-EDX), and functional groups were characterized using Attenuated Total Reflectance - Fourier Transform Infrared Spectroscopy (ATR-FTIR). Results revealed that PM2.5 particles were predominantly spherical or chain-like with carbonaceous elements (C, O, N, S), mineral dust, and trace metals. The dominant functional groups included aromatic conjugate double bond, carbonyl, and nitro group. Aqueous-phase nitration of 2-hydroxyphenol under acidic conditions, analyzed via UV-Vis spectroscopy, demonstrated an alternative nitrophenol formation pathway. Among the detected compounds, 2-hydroxyphenol and 4-nitrophenol showed the highest average concentrations (2.31±1.39) and 2.20±1.21 µg m⁻³, respectively). Seasonal variations showed elevated nitrophenol levels during winter, especially in Dhaka South (4.54±2.94 µg m⁻³). These findings highlight the quantification of phenolic precursors and the role of aqueous-phase reactions in BrC formation, providing valuable insights for future atmospheric modeling and air quality management strategies in South Asia.

Keywords: Phenolic compounds, functional groups, surface morphology, nitrophenol

50

49

26

27

28

29

30

31

32

33

34

35

36

37

38

39

40

41

42

43

44

45

46

47

48

50

1. Introduction

52

53

54

55

56

57

58

59

60

61

62

63

64

65

66

67

68

69

70

71

72

73

74

Brown carbon (BrC) is a type of organic carbon that absorbs light at shorter wavelengths, such as 300-400 nm (Laskin et al., 2015). In contrast to black carbon, brown carbon exhibits a wavelength-dependent absorptivity that increases significantly towards the higher energy end of the spectrum (Wang et al., 2023). Similar to black carbon, brown carbon (BrC) also has a positive radiative effect, which lowers the total cooling effect of atmospheric aerosols caused by light scattering (Feng et al., 2013). Because of the complexity and variety of its origins, composition, and atmospheric aging mechanisms, the direct radiative effect of BrC is still unknown despite intensive research (Lee et al., 2014). The two main sources of BrC were automobile emissions and biomass burning. The composition of primary emissions can differ significantly depending on the type of fuel and the conditions under which it burns (Laskin et al., 2015c). There are probably thousands of organic molecules in atmospheric BrC, many of which are unidentified. However, phenolic compounds are a class of components that are commonly discovered (Wang et al., 2018). Phenolic and nitrated phenols are organic substances that contain at least one hydroxyl group and a nitro group in the benzene ring. Phenolic derivatives are the major component of BrC. They originate from diverse processes of production and different emission sources. Large volumes of nitrated phenolic compounds are released into the atmosphere by primary sources such as vehicle exhaust, burning of biomass, and combustion of coal (Li et al., 2020; Wang et al., 2020). The secondary synthesis of these substances from precursors like aromatic hydrocarbons and phenolic compounds via nitration in both gaseous or aqueous phases (Harrison et al., 2005b). According to earlier research, one of the main contributors of brown carbon is nitrated phenolic compounds and R-NO₂ nitroaromatic compounds (Hossen et al., 2023; Li et al., 2022). The main reasons for the increased focus on phenolic compounds are their human toxicity (Rahman et al., 2022) and their role in producing secondary organic aerosols (SOAs) (Nakao et al., 2011). According to previous research,

phenol and cresols (such as m-cresol, p-cresol, and o-cresol) can oxidize to produce nitrophenol and its derivatives (Harrison et al., 2005). Cresols released during the burning of biomass can undergo photooxidation, producing nitro-catechol and its derivatives (Finewax et al., 2018; Iinuma et al., 2010). Furthermore, studies conducted by Andreozzi et al., (2006) and Hummel et al., (2010) have demonstrated that the primary pathway for the creation of 3-nitrosalicylic acid and 5-nitrosalicylic acid in the aqueous phase is the nitration of salicylic acid. Laboratory investigations have established the importance of aqueous processes as a production mechanism for nitrated phenolic compounds. In particular, when phenol was subjected to aqueous-phase interactions with nitronium ions (NO₂ ⁺), 4-nitrophenol was produced (Heal et al., 2007). The most prevalent nitro-aromatic species were nitrophenols and nitro catechols, which accounted for 31% and 32% of all nitro-aromatic compounds, respectively (Wang et al., 2021). To fully understand the precursor of BrC in the atmosphere, it is crucial to analyze the concentrations, chemical compositions, and sources of their phenolic precursors, along with the derivatives of nitrated and methyl derivatives of phenols. Aerosol surface morphology plays an important role in the light-absorbing properties and reactivity of BrC. Irregular or porous particle surfaces can enhance the adsorption of gaseous precursors, such as phenolic compounds, thereby influencing their heterogeneous oxidation and nitration pathways in the atmosphere. Moreover, morphological features can affect how BrC and its phenolic components interact with cloud or fog droplets, altering aqueous-phase reaction rates and the formation of light-absorbing secondary products.

75

76

77

78

79

80

81

82

83

84

85

86

87

88

89

90

91

92

93

94

95

96

97

In Bangladesh, most pollutants originate from vehicle emissions, solid waste burning, biomass burning, and brick kiln emissions (Hossain et al., 2024; Kumar et al., 2021). All these are major sources of BrC. Therefore, studies on BrC composition, such as phenolic compounds and their derivatives, in Bangladesh are essential. In previous studies, Ankhy et al., (2024); Hossen et al., (2023); and Runa et al., (2022) determined the optical properties of BrC emissions from biomass burning as well as ambient air in Dhaka,

Bangladesh, but did not investigate the individual composition of BrC. Previous studies have primarily emphasized gas-phase reactions between phenolic VOCs and NOx, followed by photochemical oxidation and subsequent partitioning into the particle phase (Hems et al., 2021; Laskin et al., 2015). Yang et al., (2021) reported that photooxidation of phenolic compounds forms BrC, and phenolic compounds are a major class of aromatic compounds known as BrC precursors. Li et al., (2020) show the formation pathway of nitro aromatic compounds via gas-phase reactions, occurring through *OH + NO2 in daytime and *NO3 + NO2 at nighttime. Our study reports an alternative pathway for the formation of nitroaromatic compounds in aqueous-phase reactions through electrophilic substitution (mediated by NO2⁺ or HONO) under acidic or alkaline conditions in the absence of sunlight, with demonstrated applicability to biomass samples. The main focus of this work, however, is the quantification of phenolic precursors of BrC. Specifically, we investigate the surface composition of PM2.5 and phenolic precursors in the atmosphere of Dhaka, Bangladesh, from July 2023 to January 2024, along with an experiment on the aqueous nitration of 2-hydroxyphenol, a common BrC precursor.

2. Methodology

2.1 Sampling sites

PM_{2.5} samples were collected from ambient air at two distinct locations in Dhaka city: Dhaka North (Shah Alibag, Mirpur-1) and Dhaka South (Department of Chemistry, University of Dhaka) (Fig. S1). Both sampling sites were situated approximately 21 meters above the ground level. The Dhaka South site, while located within an educational institution, was adjacent to a busy highway with frequent traffic congestion. Additionally, metro rail construction was ongoing nearby, further contributing to the area's pollution levels. The Dhaka North site, a mixed residential and commercial zone, was surrounded by garment factories, pharmaceutical plants, shopping centers, and restaurants. It was situated about 100 meters from the Mirpur bus station and approximately 4 kilometers from the Taltola solid waste dumping yard.

2.2 Sample Collection

PM_{2.5} samples were collected using a High-Volume Air Sampler equipped with a PM_{2.5} impactor, operating at a flow rate of 16.7 L/min, and PM_{2.5} particulates were captured on Quartz filter paper (Gelman, Membrane Filters, type TISSU Quartz 2500QAT-UP, 47 mm diameter). Before sampling, each Quartz filter was heated at 800°C for 4 hours in a furnace to remove any organic impurities. Sampling was conducted simultaneously at both locations (Dhaka South and Dhaka North sites) from July 2023 to January 2024. Each month, four samples were collected from both sites. The sampling period was 24 hours. In total, 26 samples, including blanks, were collected from each site. The PM_{2.5} mass was determined by calculating the difference between the weight of the blank filter and the PM_{2.5}-loaded filter. The total volume of air passing through the filter was calculated using the difference between the initial and final readings of the gas meter. After sampling, each sample was wrapped in aluminum foil, stored in a desiccator to regulate humidity, and finally preserved in a refrigerator at 4°C until further analysis. Flow diagrams are given below Fig.1.

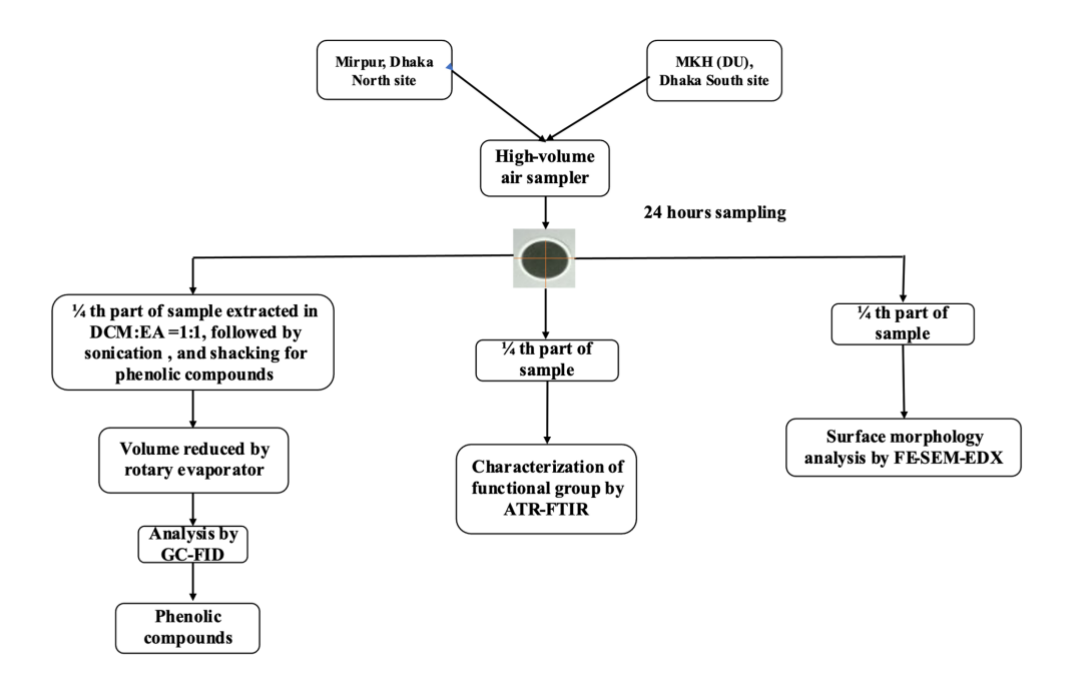


Fig. 1: Schematic diagram of the overall sampling and analysis procedure from July 2023 to January 2024 at the Dhaka North site and the Dhaka South site

Fig. 1 illustrates the sampling and analysis workflow. In short, PM_{2.5} samples were collected for 24 hours from two locations in Dhaka city. Each PM_{2.5}-loaded filter was divided into four equal parts. One-quarter was extracted and analyzed for phenolic precursors of brown carbon using gas chromatography–flame ionization detection (GC-FID). Another quarter was used to identify functional groups via attenuated total reflectance–Fourier transform infrared spectroscopy (ATR-FTIR). A further quarter was examined for surface morphology and elemental composition using field emission scanning electron microscopy coupled with energy-dispersive X-ray spectroscopy (FESEM-EDX).

2.3 SEM-EDX Analysis

Morphological and chemical analyses of PM_{2.5} were performed by field emission scanning electron microscopy (FE-SEM, Zeiss Sigma 300 VP with 2 Bruker Quantax Xflash 60 mm² SDD EDS Detectors). To obtain a high-resolution SEM image, each sample was kept in a desiccator for 1 hour and then freezedried for 6 hours to completely remove the moisture. Next, a small section of the filter was precisely severed and arranged on a sample holder using carbon nanotape. The sample surface was subjected to gold sputtering to enhance its conductivity. Due to the presence of non-conducting particles on the surface, the electron beam will collide with the sample, resulting in the accumulation of charge and causing a charging effect that leads to fuzzy pictures, which were minimized by gold sputtering. The microscope is controlled entirely by the SmartSEM software suite developed by Zeiss. After gold sputtering under reduced pressure, the sample holder was inserted into the chamber of the SEM-EDX instrument. Air from the chamber was evacuated. When the pressure was reduced below ~ 0.009 Pa, extra high tension (EHT) was enabled. SEM image was obtained with an EHT value of 2.0 kV, and EDX was performed with an EHT value ranging from 10kV -15kV. The SDD detector was utilized for EDX analysis. For obtaining the EDX report ESPRIT Spectrum software package was used. The images obtained from SEM and EDX

were analyzed by the ImageJ software package. For the morphology study, samples collected on filters may introduce positive artifacts and uncertainties due to the fiber structure of the filters. However, SEM-EDX analysis of these filter samples has been widely employed for the morphological and elemental characterization of individual airborne particles (Park et al., 2023).

2.4 ATR-FTIR analysis

An attenuated total reflection-Fourier transform infrared (ATR-FTIR) spectrometer (Shimadzu, IRPrestige-21, Japan) was utilized to examine the chemical functional group of brown carbon according to Hossen et al., (2023). IR spectra of the samples were obtained within the range of wave number 700–4000 cm⁻¹. Since an ATR probe was utilized in ATR-FTIR, sample preparation was not needed. It is a non-destructive process. During ATR-FTIR analysis, the sample was kept on the crystal (ATR probe), which is composed of high refractive index materials such as AgCl and Si. In this process, infrared (IR) radiation incident on the crystal interacts with the sample on its surface.

2.5 Sample Extraction and Chemical Analysis

To identify and quantify of phenolic precursors of BrC, half of each sample filter paper was cut into small pieces and taken into a conical flask. Then added 30.0 mL of solvent 1:1 (dichloromethane: ethylacetate) and kept it to soak overnight for better extraction. After 24 hours, each sample was sonicated for 40 min at 30°C, followed by shaking for 40 min in an orbital shaker. During the extraction process mouth of the conical flask is completely closed by a cap. The extracted solution was filtered by a syringe filter (PTFE, 0.45 µm). The volume was reduced to approximately 1.0 mL by the rotary evaporator. The final extracted samples were kept in the refrigerator at 4°C until analysis in a gas chromatography-flame ionization detector (GC-FID). The phenolic precursors of BrC in the extracted sample solutions were identified and

quantified by gas chromatography coupled with flame ionization detector (GC-FID) (model: Varian 450-184 GC, column: VF-5 ms (30m x 0.25mm, ID 0.25µm), carrier gas: N₂, Air, H₂, detector temperature: 185 280°C, Split ratio: 20, injection volume: 1.0μL, column flow: 1.2 mL/min, column temperature: Initial 186 60°C (2min hold),180°C (8°C ram/min), 180°C (10°C ram/min,) 4 min hold, total run time: 27 min). 187 Standard solution of seven phenolic compounds, such as Phenol (MERCK-Schuchardt), 2-methylphenol 188 (MERCK-Schuchardt), 3-methylphenol (MERCK-Schuchardt), 2-methoxyphenol (MERCK-189 190 Schuchardt), 2,4-dimethylphenol (MERCK-Schuchardt), 2-hydroxyphenol (MERCK-Schuchardt), 4nitrophenol (MERCK-Schuchardt) was prepared using the solvent 1:1 dichloromethane and ethylacetate. 191 Also prepared a mixed standard including these seven standard phenolic compounds. The concentrations 192 193 of the prepared standard solution were 0.5, 2.5, 5.0, 10.0, 20.0, 40.0, 60.0, 80.0, and 100.0 ppm. At first run the individual standard solution to identify the retention time of target compounds. Then the mixed 194 standard solution was injected into the gas chromatography to separate the individual phenolic 195 compounds. The presence of phenolic compounds in the ambient sample was identified by the presence 196 197 of a peak at a characteristic retention time in the sample chromatogram compared to that of the chromatogram of the standard solution. On the other hand, the quantitative analysis was conducted by 198 comparing the peak areas of the compounds to those of a standard solution, achieved through the creation 199 200 of a calibration curve (Fig.S2). Method validation, including the limit of detection (LOD), limit of 201 quantification (LOQ), and recovery rate, was also carried out for this method of quantification of phenolic 202 precursor. The details are described in the supplementary file in section 2. In a brief, the recovery experiment was carried out in three samples by spiking a known amount of standard solution. A blank 203 204 sample and the two samples that gave very little signal/peak in the chromatogram were used as a sample 205 matrix for the recovery test. A known amount of standard solutions was spiked to the filter sample and allowed the sample to stand for an hour to let the phenolic compound be absorbed into the filter matrix. 206

Then extract this spiked sample by the same process of sample extraction. The average recovery rate of the samples was 85% which is in the acceptable range (Table S1).

2.6. Correlation Analysis

The degree and direction of a linear relationship between two variables (in this case, compounds) are measured by Pearson's correlation coefficient or r. The r-value is between -1 and 1: r=1 (perfectly positive correlation), r=-1(perfectly negative correlation), r=0 no correlation. r > 0.7 means strongly correlation, 0.3 > r > 0.7 means moderately correlation, and 0.3 > r means weak correlation (Hauke and Kossowski, 2011).

2.7 Nitration Experiment of Catechol to Formation of Light-Absorbing Product

Nitrophenols are the major component of light-absorbing atmospheric organic aerosol, commonly referred as brown carbon. The primary constituent of BrC is the nitroaromatic compounds, which account for around 40-60% of the total BrC composition. Most of the nitrophenol formation pathways involve the reactions of phenolic compounds with NO₃ and NO₂ in the gas phase in the ambient atmosphere (Wang et al., 2023). Aqueous phase nitration of 1,2-dihydroxy phenol (catechol) forms a major component of brown carbon, such as 4-nitrocatechol. Catechol is produced from biomass burning and vehicle emissions. This catechol reacts with nitrous acid in the aqueous phase to form secondary aerosol nitrophenol, which is the major light-absorbing component of organic aerosol. Multiple investigations have demonstrated the significant involvement of NOx in the creation of nitroaromatic compounds (Chow et al., 2016). However, this study presents a method for the production of nitro-aromatic compounds by simple aqueous phase nitration of 2-hydroxyphenol (catechol).

Table-1: List of required reagents for the laboratory experiments to study the formation of nitro-aromatic compounds.

S/N	Reagents	Required Concentration
1.	Catechol (1,2-dihydroxybenzene), C ₆ H ₄ (OH) ₂	1 mM
2.	Sodium Nitrite, NaNO2	1 mM
3.	Sulfuric Acid, H ₂ SO ₄	0.1 M
4.	Ammonia Buffer (pH~8) & 6% H ₂ O ₂	Used for alkaline conditions
5.	Hydrogen Peroxide, H ₂ O ₂	6%

For the nitration reaction, a solution of 1 mM 1,2-dihydroxybenzene and 1 mM NaNO₂ is prepared by deionized water in a 50 mL volumetric flask. The 1:1 ratio of catechol and sodium nitrite undergoes a chemical reaction both in acidic (pH=3-4, pH adjusted by 0.1 M H₂SO₄ and NaOH) and alkaline medium (used ammonia buffer to maintain pH~9, and H₂O₂, which facilitates more NO₂⁺) to form nitrated phenol. The pH of the solution was measured by a pH meter (model L-510, voltage DC 5V, S/N PK51028202310104). During the reaction continuously measured the absorbance at different times and observed the change of absorbance with time.

239 Reaction:

OH + HO OH + H2O OH
$$(pH = 3-4)$$
 OH $(pH = 3-4)$ OH $(pH = 3-4)$ OH

3. Results and Discussion

242

243

244

245

246

247

248

249

250

251

252

253

254

255

256

257

258

259

260

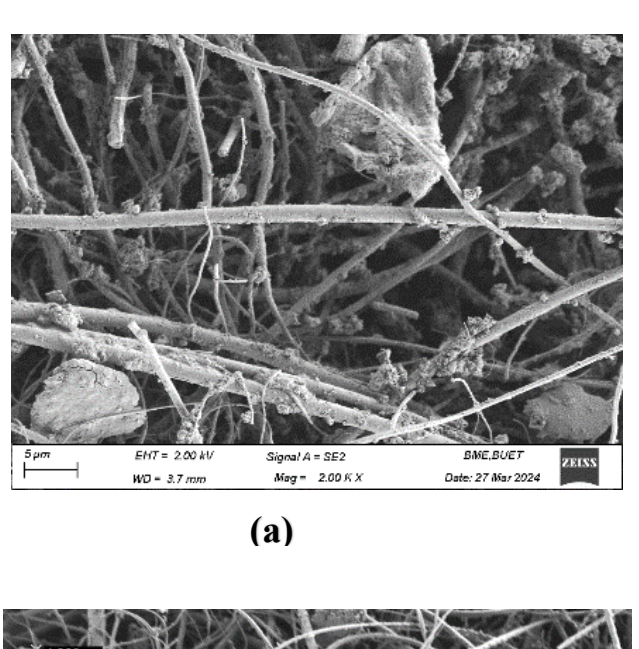
261

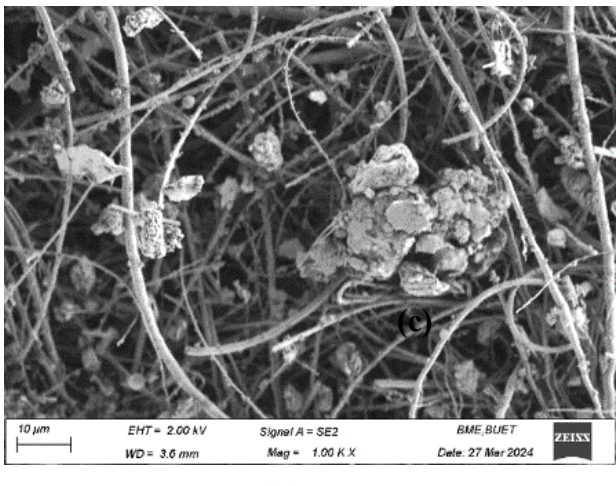
262

263

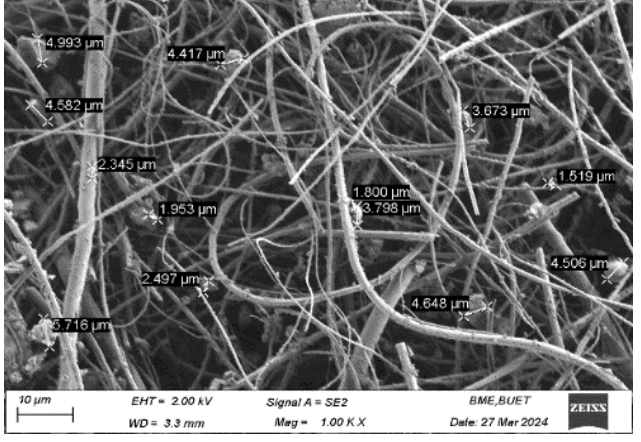
3.1 Morphological Study of PM_{2.5}

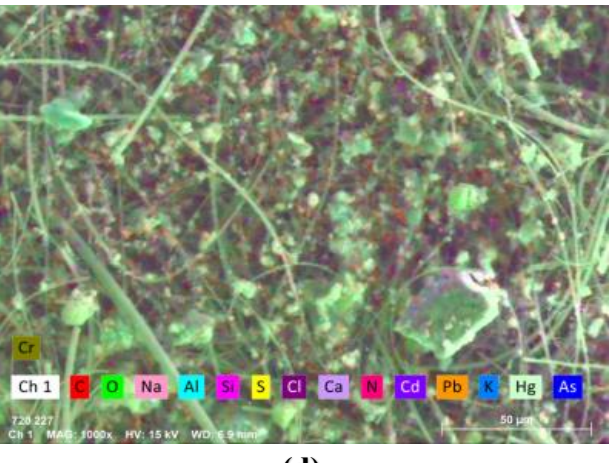
In this research investigated the surface elements that are most prevalent in the Earth's atmosphere. The chemical components of PM_{2.5} were categorized into distinct categories according to their morphology, as indicated by the SEM images (Fig. 2a-c). It shows that PM_{2.5} particles exhibit predominantly irregular, aggregate, and chain-like morphologies. Most individual particles are $\leq 2.5 \mu m$, while aggregates and chain-like structures range from 1.88 µm to 4.99 µm (Fig. 2c). Such coarse aggregates indicate particle growth through coagulation/agglomeration of smaller particles and the condensation of vapours onto preexisting seed particles, rather than formation by fresh homogeneous nucleation (Lee et al., 2019). Lots of pre-existing particles in the atmosphere are released from the combustion event of biomass in our daily life, fossil fuels, emissions from vehicles, and other sources. As a result, the gaseous pollutants in the atmosphere (NO_x, SO_x, NH₃, etc) undergo heterogeneous condensation on the surface of the pre-existing particle to form aggregates, chain-like aerosols of sulfate and nitrate. The morphology of the particles in PM_{2.5}, including diameter and shape, is similar in Dhaka North and Dhaka South sites, but the surface chemical compositions are varied with season and sampling locations. The observed surface morphologies of aerosol particles, including irregular, aggregate, and chain-like structures, play a significant role in the formation and optical properties of BrC. These morphologies provide a large reactive surface area that facilitates the heterogeneous adsorption and condensation of gaseous phenolic precursors and other organic compounds onto existing particles. Such interactions promote the chemical aging processes like nitration and oxidation, which enhance the light-absorbing capacity characteristic of BrC (Hossen et al., 2025).



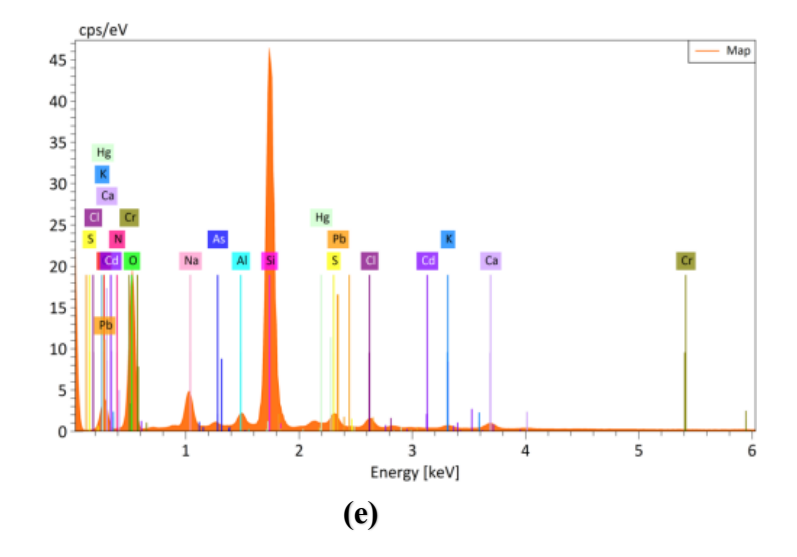


(b)





(d) (c)



Elements	Atomic	Weight
Elements	No.	%
C	12	29.84
O	16	44.61
Al	13	0.62
Na	11	2.96
K	19	0.63
N	7	0.02
\mathbf{S}	16	0.61
Ca	20	0.55
Cr	24	0.01
Pb	82	0.04
As	33	0.06
Hg	80	0.09
	(f)	

Fig. 2: Scanning Electron Microscope images of PM_{2.5} loaded filter in (a) Dhaka North site, (b) Dhaka,

South site, and (c) size distribution of particles in PM_{2.5} loaded sample; (d) Energy Dispersive X-ray

Spectroscopy mapping, (e) Spectra of PM_{2.5}, and Table (f) relative abundance of elements in PM_{2.5}

3.2 Surface Elements Analysis

According to the EDX data, surface chemical compositions were categorized into carbonaceous, mineral dust, and trace metal. Fig.2f shows that the quantity of carbon (C) and oxygen (O) was very high in PM_{2.5}, along with varying amounts of minerals (Ca, Fe, K, Al), sulfur, nitrogen, and trace metals (As, Cr, Cd, Pb, Hg). The sequence of carbonaceous elements (C, O, N, and S) in Dhaka North & South sites was O > C > N > S. Their possible emission sources are the combustion of fossil fuels and biomass burning. Sulfur dioxide (containing S) is primarily emitted from coal combustion, while nitrogen dioxide (containing N) mainly originates from agricultural land and fertilizers. The sequence of abundance for minerals is Al > Ca > K > Fe. These minerals originate from mineral dust, biomass burning, and industrial waste. The trace heavy metals were present in meager amounts. Among the five harmful trace metals (Hg, Cr, Pb, Cd, As), lead has the highest abundance of surface elements, while the abundance of Hg was the lowest. The composition suggests that particle growth was mainly due to condensation and coagulation, with mixing of combustion-related and mineral dust aerosols at the sampling sites.

3.3 Characterization of Functional Group

The IR spectra (Fig.S3) demonstrate that the majority of the material comprises the aromatic ring system because sharp peaks are found at ~ 1630-1660 cm⁻¹, and ~1440-1460 cm⁻¹. At this range, conjugated double bonds display the IR absorption. Peak obtained at 1600-1690 cm⁻¹, which is most probably the characteristic peak of stretching of the C-O-C bond. The peak at 1500-1600 cm⁻¹ suggested that the stretching of the aromatic ring, which is a common peak in all the PM_{2.5} samples (Table 2). So, it's giving

an obvious understanding that the particulate matter contains the aromatic ring with a conjugated double bond. Few samples exhibit a peak at 2400-2500 cm⁻¹ in this range -C≡N and C≡C undergo stretching vibration. The peak at the wave number 1400-1450 cm⁻¹ is the bending of methyl groups and the methylene group. Examining the fingerprint region reveals intriguing characteristics. This investigation identified a substantial number of peaks in the fingerprint region, specifically at 1325 and 1340 cm⁻¹, which indicate the existence of organic nitrate aerosol in PM_{2.5}.

Table-2: Primary band assignments for ATR-FTIR spectra of PM2.5 particulate matter

Range of Wavenumber	Vibrational Assignment
2500 – 2000 cm ⁻¹	$C \equiv N$ and $C \equiv C$ bond stretching
1800 – 1650 cm ⁻¹	Carbonyl ($C = 0$) bond stretching
1600 – 1475 cm ⁻¹	Aromatic ring stretching
1640-1550 cm ⁻¹	Bending of aromatic N-H bond
1445 cm ⁻¹	Bending of $-CH_3$, $-CH_2$ and stretching of aromatic ring
1355 – 1315 cm ⁻¹	$R - ONO_2$ organic nitrate stretching
1440 – 1220 cm ⁻¹	Bending of C-O-H
1200-1000 cm ⁻¹	Stretching vibration of $C - O$
900 – 690 cm ⁻¹	Out plane bending of aromatic ring

3.4 Identification and Quantification of Phenolic Compounds (precursor of BrC)

3.4.1 Chromatogram of GC-FID Analysis

304

305

306

307

308

309

310

311

312

313

314

315

316

317

318

319

320

321

322

323

324

325

326

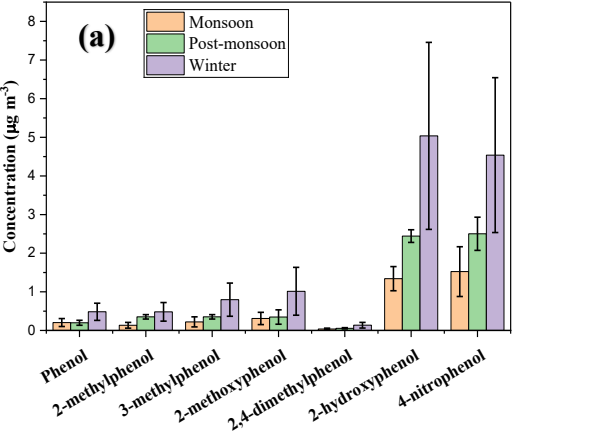
The chromatogram generated by GC-FID displayed the retention time, peak area, and identified compound. The identity of the unknown compound is ascertained through a comparison of its chromatogram with that of the standard sample. A calibration curve represents quantitative information regarding the identified compound. The chromatogram was given in the supplementary file in section 5 (Fig. S4 to S8).

3.4.2 Phenolic Precursor of BrC

The phenolic components serving as primary precursors of brown carbon include phenol, 4-nitrophenol, methoxy phenol, and cresols (m-cresol, p-cresol, and o-cresol). The precursors are initially emitted from the source as primary aerosols. Fig.3 illustrates that the mean concentration of nitrophenol and catechol in PM_{2.5} was comparatively greater than that of other phenolic compounds. The average concentrations of nitrophenol in Dhaka South (DU) during the monsoon, post-monsoon, and winter seasons were 1.52±0.64, 2.50±0.43, and 4.54±2.94 µg m⁻³, respectively. In contrast, at Mirpur, Dhaka North, the concentrations were 1.34±0.09, 1.65±0.44, and 1.62±0.52 μg m⁻³ during the same seasons. These concentrations were approximately 40-70% lower than the levels observed at the Dhaka South site. In Dhaka South, the secondhighest concentration was found to be 2-hydroxyphenol (catechol) with values of 1.34±0.31, 2.44±0.16, and 5.04±3.41 µg m⁻³ during the monsoon, post-monsoon, and winter seasons, respectively, while the values recorded at Mirpur were 1.43 ± 0.07 , 1.78 ± 0.53 , and 1.82 ± 0.51 µg m⁻³, respectively (Table S9). The levels of phenol and methyl derivatives of phenol were significantly lower compared to nitrophenol. In Mirpur, Dhaka North, the concentration of 2-hydroxyphenol is higher compared to nitrophenol. This is due to emissions from cooking, burning coal in restaurants, and biomass burning, which directly release 2-hydroxyphenol or catechol. During the winter, the increased combustion of coal and biomass for heating

purposes is responsible for the significant rises in phenolic compound concentrations (Wang et al., 2018). After the release of 2-hydroxyphenol, it undergoes a secondary chemical reaction with NOx or aqueous nitrous acid in the atmosphere to form nitrophenol.

The average concentration of phenol in Dhaka city was 0.15 ± 0.08 , 0.17 ± 0.04 , and $0.30\pm0.25~\mu g~m^{-3}$ in monsoon, post-monsoon, and winter seasons, respectively. The concentration of phenol in the winter season was comparatively higher than in other seasons because the major emission source of phenol is biomass burning. And most of the biomass burning occurred in the winter seasons. Li (2020) reported that the average concentration of phenol in urban Jinan, China was $(1.67\pm0.37)\times10^{-2}$, $(7.1\pm2.6)\times10^{-3}$, and $(2.6\pm0.4)\times10^{-3}~\mu g~m^{-3}$ in winter, spring, and summer, respectively. Among the methyl derivatives measured in Dhaka, Bangladesh, from July 2023 to January 2024, 2-methoxyphenol exhibited the highest concentration at $0.42\pm0.29~\mu g~m^{-3}$, while 2,4-dimethylphenol had the lowest concentration, recorded at $0.05\pm0.04~\mu g~m^{-3}$. The high concentration of 2-methoxyphenol, which is directly emitted from biomass burning, likely indicates frequent biomass burning activities occurring near the sampling site in Dhaka, Bangladesh.



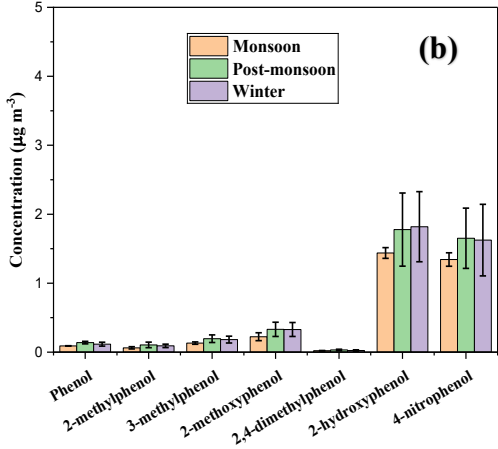


Fig. 3: Variation of concentration of phenolic compounds in (a) Dhaka, South and (b) Dhaka North site during monsoon, post-monsoon and winter

In contrast to findings from other research, the mean concentration of nitrated phenols observed in this study is significantly greater than the concentration of phenol. Li (2020) reported that the average concentration of phenol in urban Jinan, China was $(1.67 \pm 0.37) \times 10^{-2}$, $(7.1 \pm 2.6) \times 10^{-3}$, and (2.6 ± 0.4) × 10⁻³ μg m⁻³ in winter, spring, and summer, respectively. Delhomme (2010) quantified the phenolic and nitrated compounds in the ambient air and obtained the concentrations of phenol, m-cresol (3methylphenol), and o-cresol (2-methylphenol) were 1.04×10^{-2} , 2.20×10^{-3} , 1.20×10^{-3} µg m⁻³, respectively, in an urban site. Fig. 3 also shows that season and sampling location had an impact on the fractional compositions of phenolic compounds. The most prevalent phenolic compounds in PM_{2.5} during the monsoon, post-monsoon, and winter seasons were 4-nitrophenol and 2-hydroxyphenol, which accounted for 37-40% and 39-41% of the quantified phenolic precursors, respectively, in Dhaka city from July 2023 to January 2024. 2,4-dimethylphenol lies in the lowest portion among the identified phenolic compounds, accounting for 0.8-1% of the total identified phenolic precursors. The contribution of 3methylphenol increased by 0.2% from the monsoon to the post-monsoon season and saw a further increase of 0.5% during winter (Fig. 3). Previous research found that catechols and 4-nitrophenol were the most abundant phenolic compounds detected in Jinan and Beijing, with the highest observed concentrations (Wang et al., 2018; Wang et al., 2019). The prevalence of 4-nitrophenol and 2-hydroxyphenol in both Dhaka South and Dhaka North may be attributed to primary emissions, such as combustion activities, as well as the subsequent formation of precursors of BrC. The high value of nitrophenol also indicated the higher concentration of NO_x in the atmosphere. Liu et al. (2016) reported an enhancement in the light absorption of secondary organic aerosols (SOA) when exposed to elevated NO_x levels and moderate humidity, attributing this primarily to the presence of nitro-aromatic compounds as key chromophores. According to Laskin et al. (2025), the optical characteristics of brown carbon (BrC) can be altered through atmospheric aging, including

344

345

346

347

348

349

350

351

352

353

354

355

356

357

358

359

360

361

362

363

364

365

processes such as photolysis and multiphase reactions that either produce or degrade light-absorbing species.

3.4.3 Correlation analysis of phenolic compounds

Table-3: Correlation analysis of phenolic compounds

	4- NPh	2-HPh	Ph	2-MPh	3- MPh	2- MOPh	2,4- DMPh
4-NPh	1						
2-HPh	0.974	1					
Ph	0.900	0.889	1				
2-MPh	0.907	0.9199	0.9879	1			
3-MPh	0.957	0.9558	0.9813	0.9898	1		
2-MOPh	0.915	0.9442	0.966	0.9701	0.9723	1	
2,4- DMPh	0.662	0.6809	0.8341	0.8659	0.8077	0.7708	1

Note: 4-NPh= 4-nitrophenol, 2-HPh= 2-hydroxyphenol, Ph= phenol, 2-MPh= 2-methylphenol, 3-MPh= 3-methylphenol, 2-MOPh= 2-methoxyphenol, 2,4-DMPh= 2,4-dimethylphenol

The correlation analysis (Table-3) shows that most of the compounds exhibit strong correlations with each other (close to 1), indicating that they behave similarly, possibly due to shared structural or chemical properties. This analysis also indicated that most of the phenolic compounds emitted from the same sources were most probably it was biomass burning and vehicle emissions. r=0.974 for 4-NPh and 2-HPh, and r=0.9879 for Ph and 2-MPh, suggesting that an extremely strong positive correlation exists between each pair, and they behave very similarly. There is a moderate to significant association between 2,4-dimethylphenol (2,4-DMPh) and 2-methoxyphenol (2-MOPh) (r=0.7708). Their relationship is not as strongly connected as some other pairs in Table-3. 4-NPh and 2,4-DMPh show a moderate positive

correlation. They may exhibit different behaviors. 2,4-DMPh shows less correlation with other phenolic compounds.

3.5 Formation of light-absorbing nitro-aromatic compounds

In our study, we quantified several common brown carbon (BrC) precursors in the ambient atmosphere. Among them, 2-hydroxyphenol and 4-nitrophenol were found in the highest concentrations in our sampling area, both of which are well-known products of biomass burning. To gain a better understanding of the possible formation processes of nitroaromatic compounds under atmospheric conditions, we conducted controlled aqueous-phase nitration experiments in the laboratory.

In these experiments, catechol (2-hydroxyphenol), selected because it was the most abundant precursor detected in our samples, was reacted with sodium nitrite under both acidic conditions (pH adjusted using H₂SO₄ and NaOH) and basic conditions (pH adjusted using ammonia buffer, with H₂O₂ added to enhance NO₂- production) to form light absorbing nitro aromatic compound.

3.5.1. UV-visible light absorption properties of the catechol-nitrite reaction system

The catechol (2-hydroxyphenol) absorbs the UV-visible light at 280 nm (peak at 280 nm) (Scalzone et al., 2020). When it reacted with the sodium nitrite in the presence of H₂SO₄, the peak (λ_{max}) was shifted to a longer wavelength. This shift of λ_{max} indicated that there was an interaction between 2-hydroxyphenol and the nitrite ions in the reaction system (Fig. 4).

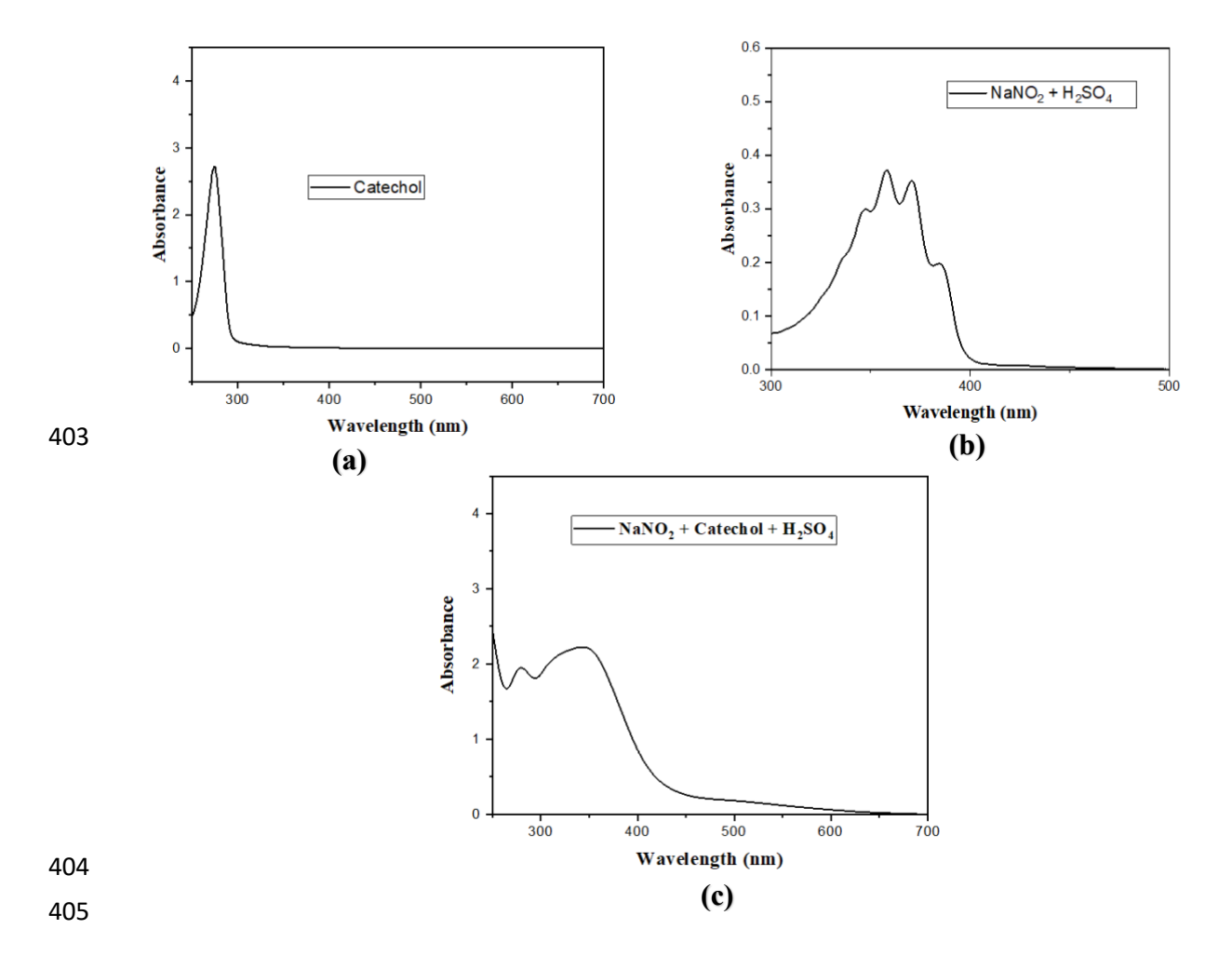
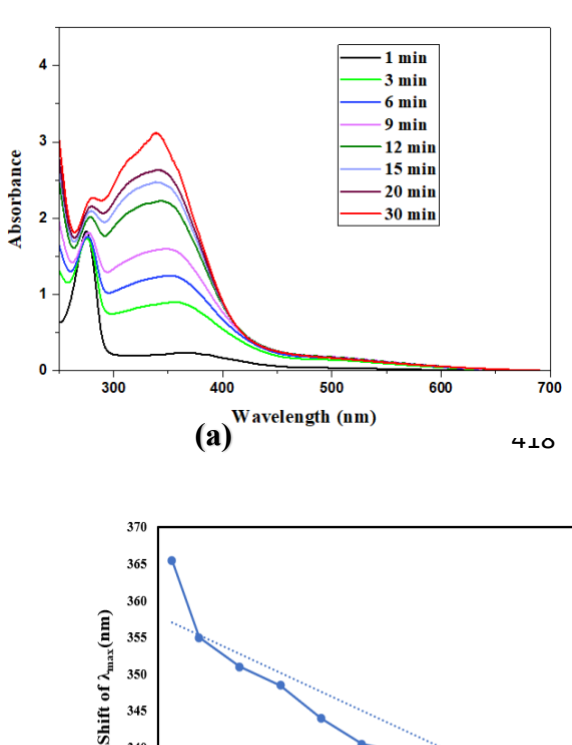


Fig. 4: Absorbance of (a) single catechol, λ_{max} =275 nm, (b) NaNO₂ + H₂SO₄, and (c) reaction system (catechol-nitrite).

Fig. 5 shows the UV–Vis spectrum of the NaNO₂ and 2-hydroxyphenol reaction system in acidic medium shows a clear time-dependent evolution in absorbance over the 1–30 min period, indicating progressive formation of new light-absorbing species. At pH=3.5, the absorbance gradually increases with time in the wavelength range from 300 – 700 nm, and the λ_{max} shifts to a shorter wavelength with time increase. Initially, at 1 min the λ_{max} obtained at 355 nm then as time increased the absorbance increased gradually and the λ_{max} shifted to a shorter wavelength such as 338 nm after half an hour and no change further increase in time (Fig.5a). It is clear from this change that the nitro group has been added to the aromatic ring, leading to an increase in absorption and a shift in the position of the peak.



Time (min)	λ _{max} (nm)	Change of absorbance
1	365.5	0.236
3	355	0.899
6	351	1.246
9	348.5	1.598
12	344	2.216
15	340.5	2.466
20	338.5	2.628
30	338	3.094

(b)

Change of absorbance 1.5 0.5 Time (min) Time (min) (d) (c)

Fig. 5: (a) Change of the absorbance with times of the reaction system containing 1 mM 2-hydroxyphenol and 1 mM NaNO₂ at pH=3.5. A distinct color denotes the duration of the sample run in the ultraviolet-visible spectrophotometer. The initial reactant contribution was subtracted from each spectrum. Table (b) Data for the shift of peak and change of absorbance, (c) Shift of λ_{max} with time, and (d) Change of absorbance with time

At the early stage (1 min), as shown in Fig. 5a, the spectrum is dominated by the characteristic $\pi \rightarrow \pi^*$ transition of the aromatic ring, centered near 270–280 nm, with relatively low intensity in the higher wavelength region. As the reaction proceeds, both the main aromatic band and a second band in the 300–350 nm region gradually increase in intensity, with the latter showing a slight bathochromic shift. This hyperchromic effect and modest red shift are consistent with the formation of nitro-substituted aromatic compounds such as o- or p-nitrophenol. The strong electron-withdrawing nature of the nitro group extends

conjugation and enhances $n\rightarrow\pi^*$ and charge-transfer transitions, leading to stronger and slightly longer wavelength absorption than the parent phenol. The continuous increase in absorbance with time, without any later decline, confirms the accumulation of these nitro-aromatic products in solution. This spectral change therefore provides strong evidence that the reaction proceeds through electrophilic aromatic substitution of 2-hydroxyphenol by nitronium ions generated from NaNO₂ in the acidic medium, yielding stable nitrophenol derivatives with enhanced UV absorption.

Reaction in alkaline medium

At high pH, nitrite remains primarily in the form of NO₂⁻, and the formation of electrophiles such as HONO, NO₂⁺, or N₂O₃ is strongly suppressed. Although phenolates are highly activating toward substitution, the lack of these electrophilic species makes aromatic nitration largely ineffective. However, the presence of peroxide facilitates the formation of NO₂⁺.

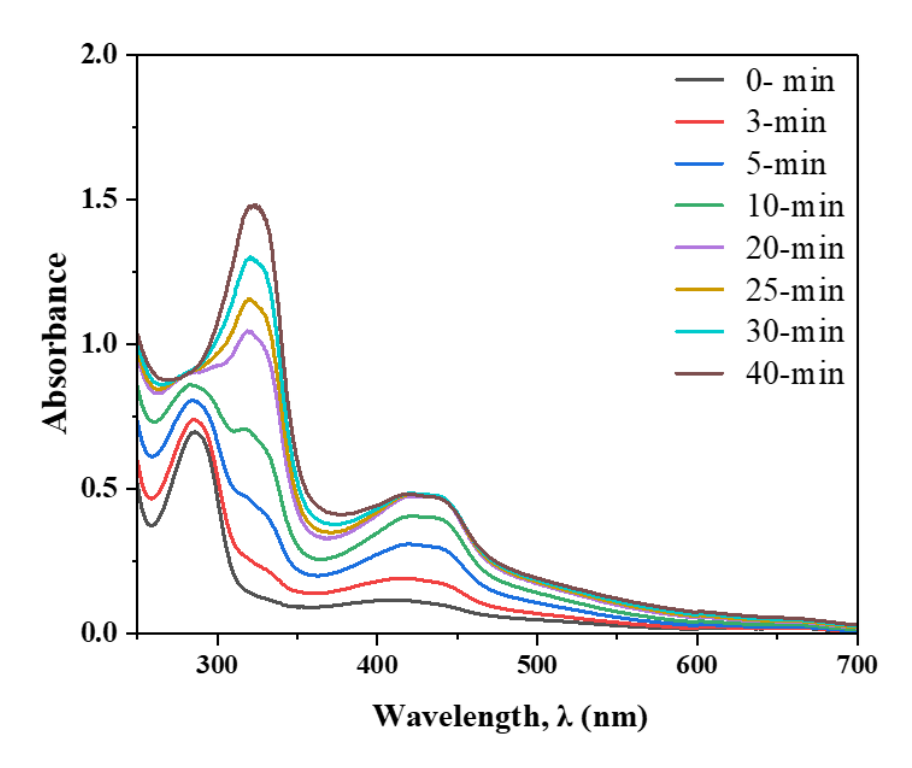


Fig. 6: UV-visible absorption spectra of the nitrite-catechol reaction system in alkaline medium, pH~7-8 to form a light-absorbing nitro aromatic compound.

Fig. 6, the UV-Vis spectra of the NaNO₂-2-hydroxyphenol system in alkaline medium with H₂O₂ show a time-dependent evolution of absorption features, indicating the formation of light-absorbing products. Initially, the spectrum is dominated by the characteristic UV absorption of phenolate anions (~280–300 nm), but with reaction time (0-15 min), the peak intensity increases and a broad shoulder emerges and intensifies in the 400–450 nm region. This indicated the completed protonated form of nitrophenol (Syedd-León et al., 2020). This bathochromic shift and visible-range growth reflect the formation of conjugated nitroaromatic and quinone-like species with extended π -systems, likely via oxidation of phenolate by HO₂-/oxidants and subsequent nitration by reactive nitrogen species from nitrite. The progressive increase in visible absorption is consistent with the generation of chromophoric, brown carbon-type products with potential atmospheric light-absorbing properties. These spectral changes strongly suggest nitro-substituted aromatic and quinone-type chromophores are forming in the system. Under acidic conditions, nitrite generates the potent electrophile NO₂⁺ (via HNO₂/HNO₂⁺) and N₂O₃/NO⁺ equilibria. The activated aromatic ring of phenol or catechol then undergoes rate-determining electrophilic attack by NO_2^+ to form the Wheland (σ) intermediate, directed ortho/para by the OH group(s). Subsequent deprotonation restores aromaticity, yielding the nitroaromatic product. The reaction mechanism of the nitration of aromatic compounds takes place through the reaction with an aqueous nitrite solution. Esteves et al., (2003) have also suggested that the exceedingly potent electrophile NO₂⁺ facilitated the reaction at a low pH. The NO₂⁺ electrophile attacks the benzene ring and forms a C-N bond. According to Wang et al., (2023) HONO acts as an electrophile in the aqueous nitration of catechol (2-hydroxybenzene). This explains the accelerated nitration rate in acidic environments, as HONO, being a stronger electrophile than NO₂-, is more readily formed at lower pH levels.

445

446

447

448

449

450

451

452

453

454

455

456

457

458

459

460

461

462

463

464

465

466

467

Under alkaline conditions, nitration is generally unfavorable. At high pH, nitrite remains primarily in the

form of NO₂⁻, and the formation of electrophiles such as HONO, NO₂⁺, or N₂O₃ is strongly suppressed.

Although phenolates are highly activating toward substitution, the lack of these electrophilic species makes aromatic nitration largely ineffective. However, the presence of peroxide facilitates the formation of NO₂⁺.

In the atmosphere, a similar pathway occurs inside aqueous aerosol droplets or cloud/fog water, where phenolic compounds (e.g., catechol) are taken up. These droplets adsorb NO₂ and interact with OH radicals under sunlight, generating reactive nitrogen species (HONO, NO₂⁺, peroxynitrite) that nitrate and oxidize the phenolic precursors. This process yields nitro-aromatic and quinone-type chromophores, which extend absorption into the visible range (Yang, X., et al. 2023). Thus, the laboratory results directly mimic the aqueous-phase reactions in atmospheric droplets that lead to the formation of light-absorbing brown carbon.

4. Conclusions

This study provides comprehensive insights into the compositions, surface elements, and formation mechanism of BrC in the atmosphere of Dhaka, Bangladesh, through the identification and quantification of seven key phenolic precursors and an aqueous-phase nitration experiment. We observed that PM_{2.5} particles predominantly exhibited spherical, irregular, and chain-like morphologies, with carbonaceous (C, O, N, S), mineral (Ca, Fe, K, Al), and trace elements (Pb, Cr, Hg, Cd, As) identified on their surfaces. ATR-FTIR analysis revealed prominent functional groups, including carbonyls, nitro groups (–NO₂), and aromatic conjugated systems, suggesting the presence of complex organic structures. Among the phenolic precursors, 4-nitrophenol (2.20±1.21 μ g m⁻³) and 2-hydroxyphenol (2.31 ± 1.39 μ g m⁻³) showed the highest concentrations, especially during winter. A strong seasonal and spatial variation was evident, with higher levels in Dhaka South, indicating the influence of urban emissions and combustion activities.

Correlation analysis revealed strong positive relationships among most compounds (r > 0.9), suggesting shared emission such biomass and fossil fuel combustion. sources as These findings suggest that phenolic compounds are not only abundant in the urban air of Dhaka but also highly reactive, forming nitrated derivatives such as 4-nitrophenol that contribute substantially to BrC. The detection of nitrated and hydroxylated phenols further highlights their transformation via atmospheric oxidation processes. The similarity in chemical behavior and high co-occurrence among these phenolic compounds confirms their common origin and potential for secondary aerosol formation.

490

491

492

493

494

495

496

497

498

499

500

501

502

503

504

505

506

507

508

509

510

511

Compared to other urban regions like Jinan, China, and Strasbourg, France, the concentrations of phenolic and nitrated phenolic compounds in Dhaka are substantially higher, likely due to more intense and unregulated combustion activities (Li et al. 2020, Delhomme et al. 2010). Our findings align with prior studies (e.g., Wang et al., 2018; Li et al., 2020) identifying catechols and nitrophenols as dominant BrC components but extend the understanding by quantifying these compounds across seasons and locations within a South Asian megacity.

While this study presents robust data on PM_{2.5} composition and BrC precursors, limitations include the relatively short sampling period and limited spatial coverage. Additionally, although aqueous-phase nitration experiments were conducted, the ambient contribution of such processes remains to be quantified. Future studies should explore broader geographic regions, perform year-round monitoring, and couple laboratory findings with atmospheric modeling for deeper mechanistic insights. The results underscore the significant contribution of phenolic and nitrated phenolic compounds to atmospheric BrC in Dhaka, with implications for both regional air quality and climate forcing. The demonstrated aqueous-phase nitration pathway of catechol at acidic pH suggests a potentially underappreciated route for BrC formation under humid and polluted conditions. This highlights the

512	importance of regulating combustion-related emissions and considering aqueous-phase chemistry in
513	climate models to accurately assess the radiative effects of organic aerosols.
544	A also avuladam aut
514	Acknowledgment
515	The authors express their gratitude to the Department of Chemistry, University of Dhaka, and the
516	Environmental and Organic Chemistry Laboratory, Chemistry Division, Atomic Energy Centre Dhaka,
517	Bangladesh
518	
519	Funding: Internal funding of the Department of Chemistry, University of Dhaka, Bangladesh
520	
521	Author's contribution
522	MAH: Conceptualization, Sampling, Methodology, Chemical analysis, Writing-original draft, Review &
523	editing
524	MHS: Chemical Analysis
525	ARMT: Chemical Analysis, Methodology, and Supervision
526	MFE: Chemical Analysis
527	AS: Conceptualization, Review & editing, Supervision
528	
529	Conflict of interest statement: The authors declared that they had no known competing financial
530	interests or personal relationships that could have appeared to influence the work reported in this paper.
531	
532	Date access statement: Data will be available upon request.

- 533 Ethics statement: The research work was done according to the ethical standard of the University of
- 534 Dhaka, Bangladesh. There is no ethical clearance was required during this research work because this
- study did not include any human and animal subjects.

536

537

5. References

- Andreozzi, R., Canterino, M., Caprio, V., Di Somma, I., and Sanchirico, R.: Salicylic acid nitration by
- means of nitric acid/acetic acid system: Chemical and kinetic characterization, Org Process Res Dev, 10,
- 540 1199–1204, https://doi.org/10.1021/op0601480, 2006.
- Ankhy, R. S., Roy, S., Nahar, A., Akbor, A., Al-amin Hossen, M., Jeba, F., Safiqul Islam, M.,
- Moniruzzaman, M., and Salam, A.: Optical Characteristics of Brown Carbon in the Atmospheric
- Particulate Matter of Dhaka, Bangladesh: Analysis of Solvent Effects and Chromophore Identification,
- 544 Heliyon, e36213, https://doi.org/10.1016/j.heliyon.2024.e36213, 2024.
- 545 Chow, K. S., Huang, X. H. H., and Yu, J. Z.: Quantification of nitroaromatic compounds in atmospheric
- 546 fine particulate matter in Hong Kong over 3 years: Field measurement evidence for secondary formation
- 547 derived from biomass burning emissions, Environmental Chemistry, 13, 665–673,
- 548 https://doi.org/10.1071/EN15174, 2016.
- 549 Delhomme, O., Morville, S., and Millet, M.: Seasonal and diurnal variations of atmospheric
- concentrations of phenols and nitrophenols measured in the Strasbourg area, France, Atmos Pollut Res, 1,
- 551 16–22, https://doi.org/10.5094/APR.2010.003, 2010.
- Esteves, P. M., Carneiro, J. W. de M., Cardoso, S. P., Barbosa, A. G. H., Laali, K. K., Rasul, G., Prakash,
- 553 G. K. S., and Olah, G. A.: Unified mechanistic concept of electrophilic aromatic nitration: Convergence
- of computational results and experimental data, J Am Chem Soc, 125, 4836–4849,
- 555 https://doi.org/10.1021/ja021307w, 2003.
- Feng, Y., Ramanathan, V., and Kotamarthi, V. R.: Brown carbon: A significant atmospheric absorber of
- solar radiation, Atmos Chem Phys, 13, 8607–8621, https://doi.org/10.5194/acp-13-8607-2013, 2013.
- 558 Finewax, Z., De Gouw, J. A., and Ziemann, P. J.: Identification and Quantification of 4-Nitrocatechol
- Formed from OH and NO3 Radical-Initiated Reactions of Catechol in Air in the Presence of NOx:
- 560 Implications for Secondary Organic Aerosol Formation from Biomass Burning, Environ Sci Technol, 52,
- 561 1981–1989, https://doi.org/10.1021/acs.est.7b05864, 2018.
- Harrison, M. A. J., Barra, S., Borghesi, D., Vione, D., Arsene, C., and Iulian Olariu, R.: Nitrated phenols
- 563 in the atmosphere: A review, Atmos Environ, 39, 231–248,
- 564 https://doi.org/10.1016/j.atmosenv.2004.09.044, 2005.

- Hauke, J. and Kossowski, T.: Comparison of values of pearson's and spearman's correlation coefficients
- on the same sets of data, Quaestiones Geographicae, 30, 87-93, https://doi.org/10.2478/v10117-011-
- 567 0021-1, 2011.
- Heal, M. R., Harrison, M. A. J., and Neil Cape, J.: Aqueous-phase nitration of phenol by N2O5 and
- 569 CINO2, Atmos Environ, 41, 3515–3520, https://doi.org/10.1016/j.atmosenv.2007.02.003, 2007.
- Hems, R. F., Schnitzler, E. G., Liu-Kang, C., Cappa, C. D., and Abbatt, J. P. D.: Aging of Atmospheric
- Brown Carbon Aerosol, https://doi.org/10.1021/acsearthspacechem.0c00346, 15 April 2021
- Hossain, M. A., Zaman, S. U., Roy, S., Islam, M. S., Zerin, I., and Salam, A.: Emission of particulate and
- 573 gaseous air pollutants from municipal solid waste in Dhaka City, Bangladesh, J Mater Cycles Waste
- 574 Manag, 26, 552–561, https://doi.org/10.1007/s10163-023-01855-w, 2024.
- Hossen, M. A. A., Roy, S., Zaman, S. U., and Salam, A.: Emission of water soluble brown carbon from
- 576 different combustion sources: Optical properties and functional group characterisation, Environ Res
- 577 Commun, 5, https://doi.org/10.1088/2515-7620/acea1d, 2023.
- Hossen, M. A. amin, Roy, S., Nahian, S., Zaman, S. U., Selim, A., and Salam, A.: Spectral characteristics
- of water-soluble Brown carbon and it's radiative impacts on the atmosphere of Dhaka, Bangladesh, Atmos
- 580 Environ, 351, 121185, https://doi.org/10.1016/J.ATMOSENV.2025.121185, 2025.
- Hummel, M., Laus, G., Nerdinger, S., and Schottenberger, H.: Improved synthesis of 3-nitrosalicylic acid,
- 582 Synth Commun, 40, 3353–3357, https://doi.org/10.1080/00397910903419852, 2010.
- 583 Iinuma, Y., Böge, O., and Herrmann, H.: Methyl-nitrocatechols: Atmospheric tracer compounds for
- 584 biomass burning secondary organic aerosols, Environ Sci Technol, 44, 8453-8459,
- 585 https://doi.org/10.1021/es102938a, 2010.
- Kulmala, M., Dal Maso, M., Ma"kela", J. M., Ma"kela, M., Ma"kela", M., Pirjola, L., Va"keva", Va", M.,
- Va"keva", V., Aalto, V. P., Miikkulainen, P., Ha"meri, K., Ha"meri, H., and O'dowd, C. D.: On the
- formation, growth and composition of nucleation mode particles, 53, 479–490, 2001.
- Kumar, P., Hama, S., Nogueira, T., Abbass, R. A., Brand, V. S., Andrade, M. de F., Asfaw, A., Aziz, K.
- 590 H., Cao, S. J., El-Gendy, A., Islam, S., Jeba, F., Khare, M., Mamuya, S. H., Martinez, J., Meng, M. R.,
- Morawska, L., Muula, A. S., Shiva Nagendra, S. M., Ngowi, A. V., Omer, K., Olaya, Y., Osano, P., and
- 592 Salam, A.: In-car particulate matter exposure across ten global cities, Science of the Total Environment,
- 593 750, https://doi.org/10.1016/j.scitotenv.2020.141395, 2021.
- 594 Laskin, A., Laskin, J., and Nizkorodov, S. A.: Chemistry of Atmospheric Brown Carbon,
- 595 https://doi.org/10.1021/cr5006167, 27 May 2015.
- Laskin, A., West, C. P., and Hettiyadura, A. P. S.: Molecular insights into the composition, sources, and
- aging of atmospheric brown carbon, https://doi.org/10.1039/d3cs00609c, 2 January 2025.
- Lee, H. J., Aiona, P. K., Laskin, A., Laskin, J., and Nizkorodov, S. A.: Effect of solar radiation on the
- optical properties and molecular composition of laboratory proxies of atmospheric brown carbon, Environ
- 600 Sci Technol, 48, 10217–10226, https://doi.org/10.1021/es502515r, 2014.

- Lee, S. H., Gordon, H., Yu, H., Lehtipalo, K., Haley, R., Li, Y., and Zhang, R.: New Particle Formation
- in the Atmosphere: From Molecular Clusters to Global Climate, https://doi.org/10.1029/2018JD029356,
- 603 16 July 2019.
- Li, M., Wang, X., Lu, C., Li, R., Zhang, J., Dong, S., Yang, L., Xue, L., Chen, J., and Wang, W.: Nitrated
- 605 phenols and the phenolic precursors in the atmosphere in urban Jinan, China, Science of the Total
- 606 Environment, 714, https://doi.org/10.1016/j.scitotenv.2020.136760, 2020.
- 607 Li, M., Wang, X., Zhao, Y., Du, P., Li, H., Li, J., Shen, H., Liu, Z., Jiang, Y., Chen, J., Bi, Y., Zhao, Y.,
- Xue, L., Wang, Y., Chen, J., and Wang, W.: Atmospheric Nitrated Phenolic Compounds in Particle,
- 609 Gaseous, and Aqueous Phases During Cloud Events at a Mountain Site in North China: Distribution
- 610 Characteristics and Aqueous-Phase Formation, Journal of Geophysical Research: Atmospheres, 127,
- 611 https://doi.org/10.1029/2022JD037130, 2022.
- Nakao, S., Clark, C., Tang, P., Sato, K., and Cocker, D.: Secondary organic aerosol formation from
- 613 phenolic compounds in the absence of NOx, Atmos Chem Phys, 11, 10649-10660,
- 614 https://doi.org/10.5194/acp-11-10649-2011, 2011.
- Park, J. I., Kim, M. S., Yeo, M., Choi, M., Lee, J. Y., Natsagdori, A., Kim, C., Song, M., and Jang, K. S.:
- 616 Chemical and morphological characterization by SEM-EDS of PM2.5 collected during winter in
- Ulaanbaatar, Mongolia, Atmos Environ, 303, https://doi.org/10.1016/j.atmosenv.2023.119752, 2023.
- Rahman, M. M., Rahaman, M. S., Islam, M. R., Rahman, F., Mithi, F. M., Alqahtani, T., Almikhlafi, M.
- A., Alghamdi, S. Q., Alruwaili, A. S., Hossain, M. S., Ahmed, M., Das, R., Emran, T. Bin, and Uddin, M.
- 620 S.: Role of phenolic compounds in human disease: Current knowledge and future prospects,
- 621 https://doi.org/10.3390/molecules27010233, 1 January 2022.
- Runa, F., Islam, M. S., Jeba, F., and Salam, A.: Light absorption properties of brown carbon from biomass
- 623 burning emissions, Environmental Science and Pollution Research, 29, 21012–21022,
- 624 https://doi.org/10.1007/s11356-021-17220-z, 2022.
- 625 Scalzone, A., Bonifacio, M. A., Cometa, S., Cucinotta, F., De Giglio, E., Ferreira, A. M., and Gentile, P.:
- 626 pH-Triggered Adhesiveness and Cohesiveness of Chondroitin Sulfate-Catechol Biopolymer for
- Biomedical Applications, Front Bioeng Biotechnol, 8, https://doi.org/10.3389/fbioe.2020.00712, 2020.
- 628 Wang, H., Gao, Y., Wang, S., Wu, X., Liu, Y., Li, X., Huang, D., Lou, S., Wu, Z., Guo, S., Jing, S., Li,
- Y., Huang, C., Tyndall, G. S., Orlando, J. J., and Zhang, X.: Atmospheric Processing of Nitrophenols and
- Nitrocresols From Biomass Burning Emissions, Journal of Geophysical Research: Atmospheres, 125,
- 631 https://doi.org/10.1029/2020JD033401, 2020.
- 632 Wang, J., Nie, W., Cheng, Y., Shen, Y., Chi, X., Wang, J., Huang, X., Xie, Y., Sun, P., Xu, Z., Qi, X., Su,
- H., and Ding, A.: Light absorption of brown carbon in eastern China based on 3-year multi-wavelength
- 634 aerosol optical property observations and an improved absorption Ångström exponent segregation
- 635 method, Atmos Chem Phys, 18, 9061–9074, https://doi.org/10.5194/acp-18-9061-2018, 2018a.
- 636 Wang, L., Wang, X., Gu, R., Wang, H., Yao, L., Wen, L., Zhu, F., Wang, W., Xue, L., Yang, L., Lu, K.,
- 637 Chen, J., Wang, T., Zhang, Y., and Wang, W.: Observations of fine particulate nitrated phenols in four

- 638 sites in northern China: Concentrations, source apportionment, and secondary formation, Atmos Chem
- Phys, 18, 4349–4359, https://doi.org/10.5194/acp-18-4349-2018, 2018b.
- 640 Wang, Y., Hu, M., Wang, Y., Zheng, J., Shang, D., Yang, Y., Liu, Y., Li, X., Tang, R., Zhu, W., Du, Z.,
- Wu, Y., Guo, S., Wu, Z., Lou, S., Hallquist, M., and Yu, J. Z.: The formation of nitro-aromatic compounds
- under high NOx and anthropogenic VOC conditions in urban Beijing, China, Atmos Chem Phys, 19,
- 7649–7665, https://doi.org/10.5194/acp-19-7649-2019, 2019.
- Wang, Y., Jorga, S., and Abbatt, J.: Nitration of Phenols by Reaction with Aqueous Nitrite: A Pathway
- 645 for the Formation of Atmospheric Brown Carbon, ACS Earth Space Chem, 7, 632-641,
- 646 https://doi.org/10.1021/acsearthspacechem.2c00396, 2023.
- Wang, Z., Zhang, J., Zhang, L., Liang, Y., and Shi, Q.: Characterization of nitroaromatic compounds in
- 648 atmospheric particulate matter from Beijing, Atmos Environ, 246,
- 649 https://doi.org/10.1016/j.atmosenv.2020.118046, 2021.
- Yang, J., Au, W. C., Law, H., Lam, C. H., and Nah, T.: Formation and evolution of brown carbon during
- agueous-phase nitrate-mediated photooxidation of guaiacol and 5-nitroguaiacol, Atmos Environ, 254,
- 652 https://doi.org/10.1016/j.atmosenv.2021.118401, 2021.